GPCR SIGNALING

Genetic evidence that β-arrestins are dispensable for the initiation of β2-adrenergic receptor signaling to ERK

Morgan O'Hayre,[1] Kelsie Eichel,[2]* Silvia Avino,[1,3]* Xuefeng Zhao,[1,4,5] Dana J. Steffen,[4] Xiaodong Feng,[1,4] Kouki Kawakami,[6] Junken Aoki,[6,7] Karen Messer,[4] Roger Sunahara,[4] Asuka Inoue,[6,8] Mark von Zastrow,[2,9] J. Silvio Gutkind[1,4†]

The β2-adrenergic receptor (β2AR) has provided a paradigm to elucidate how G protein–coupled receptors (GPCRs) control intracellular signaling, including the discovery that β-arrestins, which bind to ligand-activated GPCRs, are central for GPCR function. We used genome editing, conditional gene deletion, and small interfering RNAs (siRNAs) to determine the roles of β-arrestin 1 (β-arr1) and β-arr2 in β2AR internalization, trafficking, and signaling to ERK. We found that only β-arr2 was essential for β2AR internalization. Unexpectedly, β-arr1 and β-arr2 and receptor internalization were dispensable for ERK activation. Instead, β2AR signaled through Gαs and Gβγ subunits through a pathway that involved the tyrosine kinase SRC, the adaptor protein SHC, the guanine nucleotide exchange factor SOS, the small GTPase RAS, and the kinases RAF and MEK, which led to ERK activation. These findings provide a molecular framework for β2AR signaling through β-arrestin–independent pathways in key physiological functions and under pathological conditions.

INTRODUCTION

G protein (heterotrimeric guanine nucleotide–binding protein)–coupled receptors (GPCRs) represent the largest family of cell surface proteins involved in signal transmission. These receptors play key roles in physiological processes, and their dysfunction contributes to some of the most prevalent human diseases (1). Hence, GPCRs are the direct or indirect target of more than 25% of drugs on the market (1, 2). The study of β2-adrenergic receptors (β2ARs) has provided a paradigm to elucidate the fundamental mechanisms by which GPCRs control intracellular signaling in key physiological functions and under pathological conditions (1, 3–7).

Upon ligand binding, β2AR undergoes a rapid conformational change, leading to its association with the Gα subunit of the heterotrimeric G protein G_s (Gαs) and the consequent release of guanosine diphosphate bound to Gαs and its exchange for guanosine triphosphate (GTP) (3, 6, 7). Whereas GTP-Gαs initiates signal transmission resulting in 3′,5′-cyclic adenosine monophosphate (cAMP) accumulation, G protein–coupled receptor kinases (GRKs) phosphorylate the C terminus of β2AR (5). This leads to recruitment of β-arrestins, which associate with β2ARs and cause receptor desensitization by uncoupling receptors from G proteins and promoting their internalization through clathrin-coated pits (4, 5, 8, 9), resulting in G protein signal termination at the plasma membrane. In addition to desensitization of G protein signaling, β-arrestins

have also been proposed to initiate their own signals that stimulate the mitogen-activated protein kinases (MAPKs) extracellular signal–regulated kinase 1/2 (ERK1/2) (collectively referred herein as ERK) (8, 9). However, the respective roles of β-arrestin 1 (β-arr1) and β-arr2 (also known as arrestin-2 and arrestin-3, respectively) in receptor internalization and ERK activation have not been fully elucidated (10), and the relative contribution of β-arrestins and Gαs to overall ERK activation by β2AR has been debated (9, 11, 12). This has hindered a thorough mechanistic understanding of how β2AR activates ERK and hence limited the full potential of interfering with GPCR signaling to ERK for therapeutic intervention in multiple diseases.

RESULTS

β-arr2, but not β-arr1, is essential for β2AR internalization

To begin investigating the relative contributions of β-arr1 and β-arr2 to receptor internalization and signaling and the potential for redundancy, we established flow cytometry assays to determine the cell surface amounts of FLAG-β2AR upon activation by its agonist, isoproterenol. Internalization of stably expressed FLAG-β2AR in human embryonic kidney (HEK) 293 cells occurred rapidly, reaching a maximum within 15 to 30 min (Fig. 1, A to C). A phosphorylation-deficient mutant FLAG-β2AR 3S, in which the C-terminal GRK phosphorylation sites were mutated to impair β-arrestin–induced desensitization and internalization (13), showed minimal isoproterenol-stimulated receptor internalization, thus serving as a control (Fig. 1, A to C). Similarly, stimulation of cells at 4°C completely abolished receptor internalization (Fig. 1, B and C). As an additional control, the constitutive uptake of fluorescently labeled transferrin was monitored in HEK293 FLAG-β2AR and FLAG-β2AR 3S cell lines, which showed no significant differences (fig. S1A). To evaluate β-arrestin function in β2AR internalization, we performed small interfering RNA (siRNA) knockdown in HEK293 FLAG-β2AR cells (Fig. 1D). Knockdown of β-arr1 alone had little effect on receptor internalization compared with siRNA control (siCont) (Fig. 1E). However, knockdown of β-arr2 alone largely impaired β2AR internalization, similar to knockdown of both β-arr1 and β-arr2, suggesting an important role for β-arr2,

[1]Oral and Pharyngeal Cancer Branch, National Institute of Dental and Craniofacial Research, National Institutes of Health, Bethesda, MD 20852, USA. [2]Department of Psychiatry, University of California, San Francisco, San Francisco, CA 94158, USA. [3]Department of Pharmacy, Health and Nutritional Sciences, University of Calabria, Via Pietro Bucci, 87036 Rende (CS), Italy. [4]Department of Pharmacology and Moores Cancer Center, University of California, San Diego, La Jolla, CA 92093, USA. [5]State Key Laboratory of Oral Diseases, National Clinical Research Center for Oral Diseases, West China Hospital of Stomatology, Sichuan University, Chengdu, China. [6]Graduate School of Pharmaceutical Sciences, Tohoku University, Aoba-ku, Sendai, Miyagi 980-8578, Japan. [7]Japan Agency for Medical Research and Development, Core Research for Evolutional Science and Technology, Chiyoda-ku, Tokyo 100-0004, Japan. [8]Japan Science and Technology Agency, Precursory Research for Embryonic Science and Technology, Kawaguchi, Saitama 332-0012, Japan. [9]Department of Cellular and Molecular Pharmacology, University of California, San Francisco, San Francisco, CA 94158, USA.
*These authors contributed equally to this work.
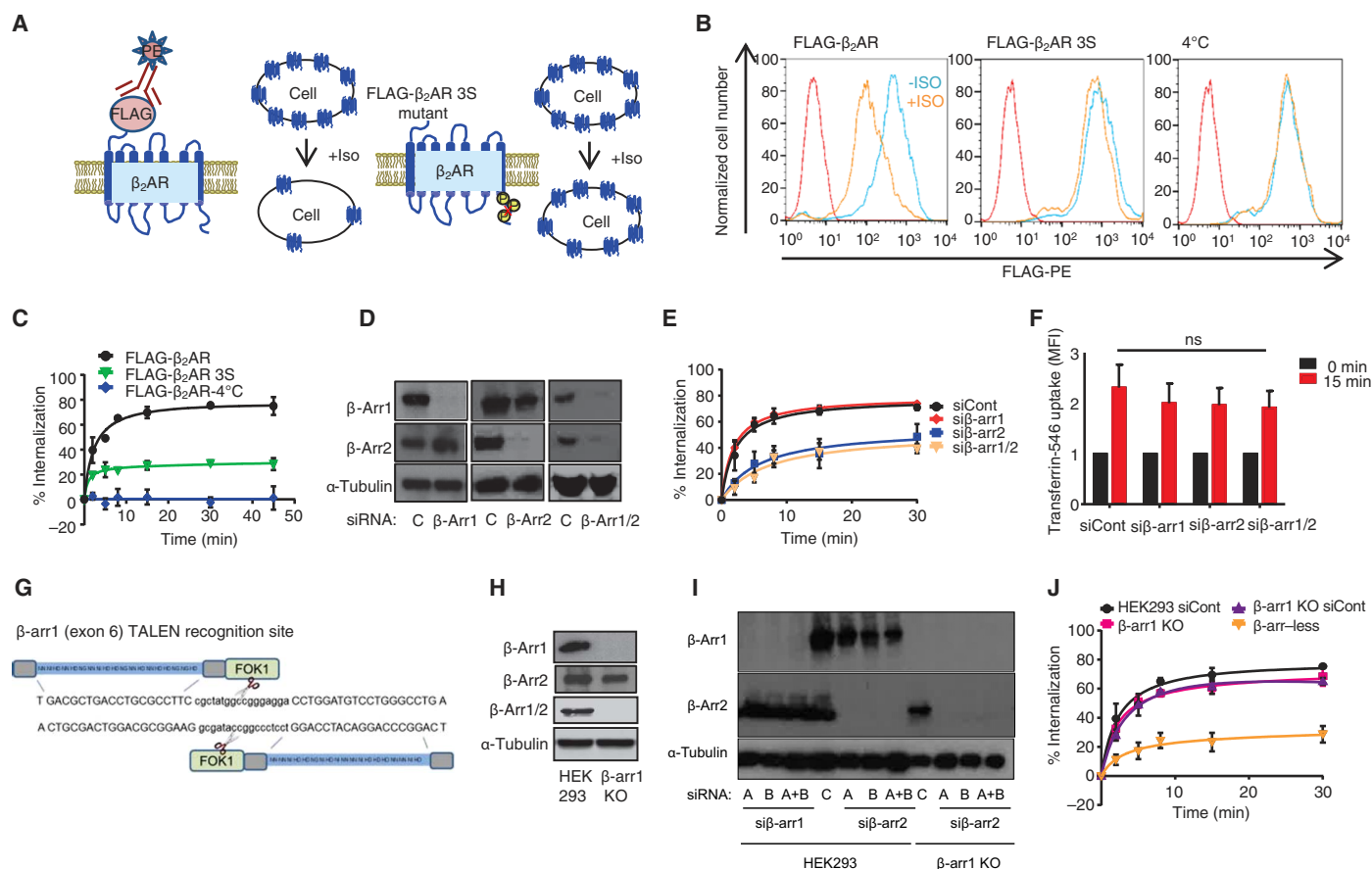†Corresponding author. Email: sgutkind@ucsd.edu

Fig. 1. Internalization of β2AR in HEK293, β-arr1 KO, and β-arr–less cells. (**A**) Schematic of FLAG-β2AR and FLAG-β2AR 3S internalization assays. Iso, isoproterenol. (**B**) Surface FLAG-β2AR or FLAG-β2AR 3S abundance in HEK293 cells before or after 15 min of isoproterenol (10 μM) stimulation compared with isotype-stained reference control and control stimulation at 4°C. (**C**) Internalization of FLAG-β2AR or FLAG-β2AR 3S after isoproterenol stimulation; mean of three independent experiments as in (B) ± SD. (**D**) Western blot of β-arr1 and β-arr2 and α-tubulin (loading control) in HEK293 cells transfected with β-arrestin or control siRNAs (C). Representative of four independent experiments. (**E**) Internalization of FLAG-β2AR after isoproterenol stimulation in HEK293 cells transfected with β-arrestin or control siRNAs; mean of three independent experiments ± SD. (**F**) Flow cytometry quantification of median fluorescence intensity (MFI) of 15-min transferrin-546 uptake in HEK293 FLAG-β2AR cells transfected with control siRNA (siCont) or indicated siRNAs; mean of three independent experiments ± SD. ns, not significant. (**G**) Schematic of the β-arr1 TALEN construct design targeting exon 6. (**H** and **I**) Western blot for β-arrestins in (H) HEK293 and β-arr1 KO cells and in (I) HEK293 and β-arr1 KO cells transfected with two different siRNAs (A, B) targeting β-arr1 or β-arr2 or siRNA pools (A + B) or control scrambled siRNA (C). (**J**) Internalization of FLAG-β2AR after isoproterenol stimulation in indicated cells; mean of three independent experiments ± SD.

but not β-arr1, in β2AR internalization (Fig. 1E). Transferrin uptake was similar under all conditions (Fig. 1F).

Advances in genome editing strategies with the development of TALEN (transcription activator–like effector nucleases) and CRISPR (clustered regularly interspaced short palindromic repeats) techniques have now made it feasible to investigate the effects of precise gene deletion (*14*, *15*), as opposed to relying entirely on transient siRNA knockdown approaches. We used TALEN genome editing targeting β-arr1 to generate a β-arr1 knockout (KO) HEK293 cell line (Fig. 1, G and H, and fig. S1B). An antibody that detects both β-arr1 and β-arr2 did not yield a signal in the β-arr1 KO line, which agreed with previous reports that β-arr1 is generally more highly abundant (*16*, *17*). Nevertheless, the use of a β-arr2–specific antibody indicated the presence of β-arr2 in both the parental HEK293 and β-arr1 KO lines (Fig. 1H). Two independent siRNAs targeting each β-arrestin effectively knocked down their respective target proteins, and the siRNAs were pooled for further experiments that compared the effects of β-arr1 or β-arr2. The

β-arr1 KO cells transfected with the pool of siRNAs targeting β-arr2 were henceforth designated β-arr–less cells (Fig. 1I). Similar to the siRNA knockdown approach, the HEK293 β-arr1 KO cells expressing FLAG-β2AR had similar β2AR internalization patterns as the HEK293 FLAG-β2AR control cells (Fig. 1J). However, the loss of β-arr2 in the β-arr–less cells greatly impaired β2AR internalization (Fig. 1J) without affecting transferrin uptake (fig. S1C).

β-arr2 is required for β2AR trafficking to clathrin-coated pits and internalization into endocytic vesicles

We next took advantage of the use of the SNAP-tag system to specifically label cell surface–expressed β2AR to visualize the internalization process by live cell confocal imaging and immunofluorescence of fixed cells (Fig. 2A). Aligning with our observations by flow cytometry internalization analysis using FLAG-β2AR cells, HEK293 and β-arr1 KO cells readily internalized SNAP-labeled β2AR into early endosomes upon stimulation with isoproterenol (Fig. 2B and movies S1 and S2). However, SNAP-β2AR predominantly remained
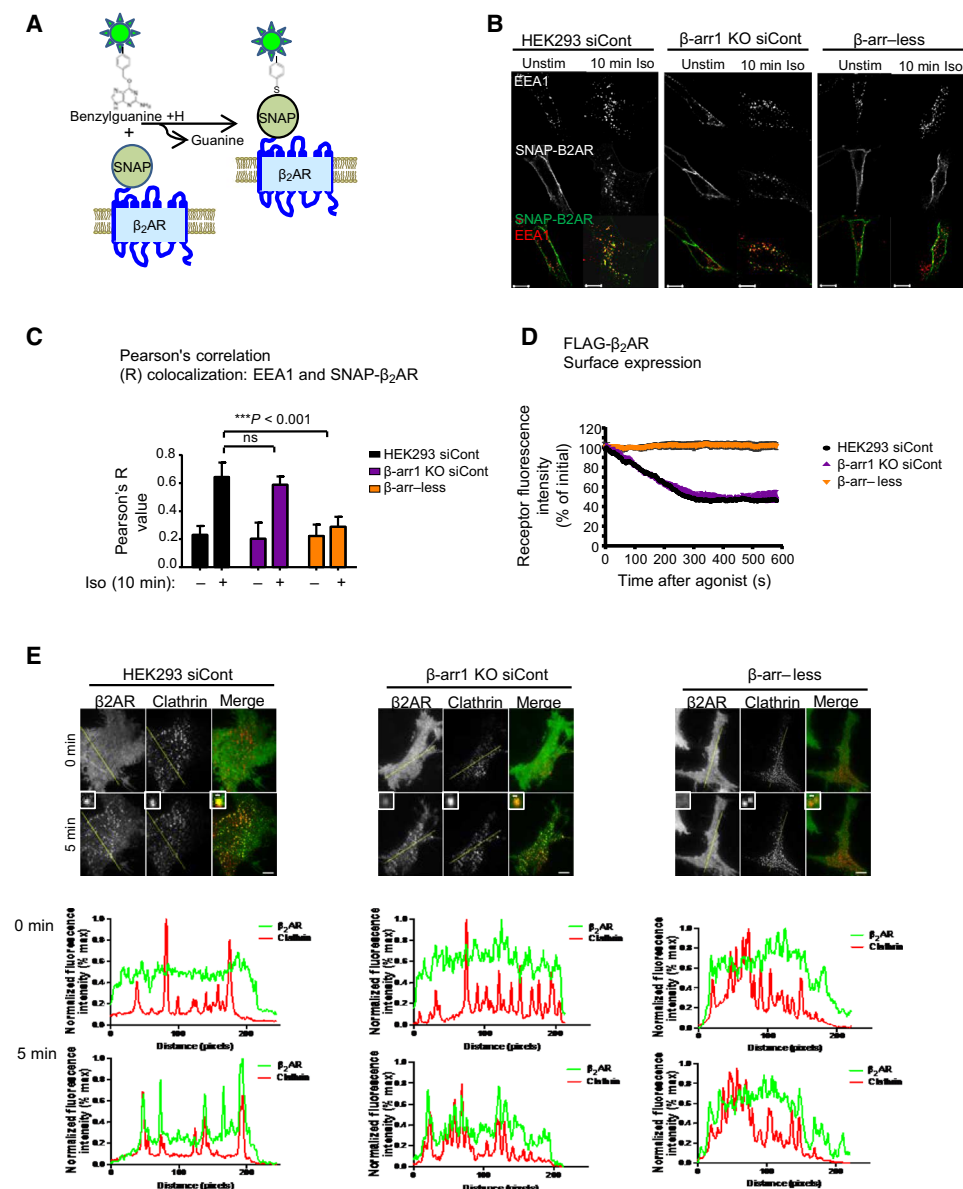
Fig. 2. β₂AR internalization into endocytic vesicles through clathrin-coated pits. (**A**) Schematic of SNAP-tagged β₂AR used for immunofluorescence (IF) imaging. Immunofluorescence of SNAP-β₂AR and EEA1 endocytic vesicles (**B**) and respective Pearson's correlation (R) values (**C**). Mean of 12 individual cells imaged from two independent experiments ± SEM in the indicated cells upon 10-min isoproterenol stimulation. Statistical significance was determined by t test. Scale bars, 10 μm. (**D**) Surface FLAG-β₂AR abundance in the indicated cells after isoproterenol stimulation, determined by TIRF microscopy using fluorescently labeled β-arr2 siRNA. Representative of three independent experiments. (**E**) TIRF imaging of FLAG-β₂AR (green) and clathrin-coated pits (red) in indicated cells before and after 5-min isoproterenol stimulation. Graphs depict the overlap in fluorescence intensity between FLAG-β₂AR and clathrin-coated pits across designated lines through the cells, as an indication of colocalization. Scale bars, 5 μm; inset scale bars, 500 nm. Representative of three independent experiments.

on the cell surface in β-arr–less cells (Fig. 2B and movie S3). Immunofluorescence analysis with the early endosome marker EEA1 revealed that SNAP-β₂AR colocalized with EEA1 in early endosomes in isoproterenol-stimulated control cells and β-arr1 KO cells, but not in β-arr–less cells, as quantified by Pearson's coefficient analysis (Fig. 2, B and C).

We verified by total internal reflection fluorescence (TIRF) microscopy that FLAG-β₂AR endocytosis was abolished in β-arr–less

cells (Fig. 2D), whereas β-arr1 KO cells maintained similar amounts of internalization compared with control HEK293 cells, in agreement with the flow cytometry and immunofluorescence data. We then examined β₂AR accumulation in clathrin-coated pits, the key step in the process of ligand-induced endocytosis of β₂AR that is promoted by β-arrestins. β₂AR clustered rapidly in clathrin-coated pits after isoproterenol application in HEK293 and β-arr1 KO cells, whereas receptor clustering in clathrin-coated pits was abolished in β-arr–less cells (Fig. 2E, fig. S2A, and movies S4 to S6). Additionally, knockdown of clathrin heavy chain disrupted FLAG-β₂AR internalization, verifying that β₂AR internalization was clathrin-dependent in these cells (fig. S2B). Thus, our data obtained through multiple complementary approaches indicate that β₂AR internalization occurs predominantly through clustering of receptors into clathrin-coated pits that is specifically β-arr2–dependent.

β-arrestins are dispensable for ERK activation

In addition to receptor internalization, β-arrestins are proposed to desensitize β₂AR signaling while concomitantly initiating β-arrestin–dependent signaling to ERK (9, 11, 18). Strikingly, the β-arr–less cells did not show decreased ERK phosphorylation but instead showed increased ERK activation in response to β₂AR stimulation when compared with control HEK293 cells, using both In-Cell Western (Fig. 3A) and traditional Western blot (Fig. 3B) approaches. Although these results were unexpected, ERK activation was similarly increased rather than decreased in cells expressing the FLAG-β₂AR 3S mutant that had impaired internalization and β-arrestin recruitment (Figs. 1, A to C, and 3, C to E). These data collectively suggest that initiation of ERK signaling from β₂AR does not require receptor internalization or β-arrestins.

The enhanced signaling from β₂AR to ERK in β-arr–less cells was confirmed by the increased sensitivity to the synthetic (isoproterenol) and natural (epinephrine) β₂AR agonists by Western blot and phosphorylated ERK enzyme-linked immunosorbent assay (ELISA) analysis of dose-response curves. This approach revealed higher maximal responses (E_{max}) and lower median effective concentration (EC_{50}) values in β-arr–less cells compared with control cells (Fig. 3F). We also investigated the effects of β-arrestin depletion on cAMP signaling. Both β-arr2 knockdown and β-arr1 KO cells had increased cAMP production in

response to isoproterenol that was greater in the β-arr–less cells (fig. S3). These data support the idea that β-arrestins restrain β$_2$AR-initiated ERK activation and cAMP accumulation. Moreover, we also used the CRISPR/Cas9 system to genetically delete both β-arr1 and β-arr2 simultaneously (Fig. 3G and fig. S4, A to D). Similar to the β-arr–less cells, two separate β-arr1/2 double-KO clonal cells showed stronger phosphorylation of ERK at early time points compared with the parental control cells (Fig. 3H). This complementary genome editing approach provided further support to the notion that β-arrestins are dispensable for ERK activation by β$_2$AR. The amounts of endogenous and transfected β$_2$AR were similar between parental HEK293 and β-arr1/2 KO cell lines, as measured by specific binding of [^{3}H]dihydroalprenolol ([^{3}H]DHAP), suggesting that differences in receptor amounts did not account for the differences in signaling observed (fig. S5A). Furthermore, we verified that the β-arr1/2 double-KO lines had abolished β$_2$AR and arginine vasopressin receptor 2 (V2R) internalization upon stimulation with their respective ligands, isoproterenol and arginine vasopressin (AVP) (fig. S5, B and C). These observations were consistent with an important role for β-arr2 in receptor-mediated internalization (Figs. 1 and 2). We also observed an increase in isoproterenol-mediated ERK activation in β-arr1/2 double-KO lines relative to the parental HEK293 cells with endogenous receptor amounts (Fig. 3I), suggesting that receptor overexpression was not affecting the results. In addition, we compared the effects of the loss of β-arr1/2 on ERK activation by another GPCR, V2R. Similar to results observed with β$_2$AR, β-arr1/2 was dispensable for V2R-mediated ERK activation (fig. S6).

ERK activation by β$_2$AR is Gα$_s$-dependent

β$_2$AR is predominantly coupled to Gα$_s$. Thus, in the search for the underlying mechanism(s) linking β$_2$AR to ERK, we tested whether Gα$_s$ coupling was required for isoproterenol-mediated ERK phosphorylation. Using mouse embryonic fibroblasts (MEFs) derived from *Gnas*$^{f/f}$ mice, we generated a stable FLAG-β$_2$AR–expressing cell line (fig. S7A). Cells infected with control adenovirus exhibited a robust activation of ERK, whereas excision of Gα$_s$ using a Cre–green fluorescent protein (GFP) adenovirus abrogated isoproterenol-induced ERK phosphorylation (Fig. 4A). Thus, conditional Gα$_s$ gene deletion eliminated ERK activation in MEFs. As a complementary approach, we used G$_s$-deleted HEK293 cells lacking both of the expressed Gα$_s$ gene members (*GNAS* and *GNAL*), generated using the CRISPR/Cas9 system (Fig. 4B and fig. S7B). Compared with the parental cells, the *GNAS* KO HEK293 cells had nearly complete impairment of ERK activation by isoproterenol, whereas control epidermal growth factor (EGF)–mediated activation of ERK was preserved (Fig. 4C). Disruption of Gα$_s$ signaling in these cells was confirmed by cAMP and CRE luciferase assays and by its restoration by Gα$_s$ reexpression (Fig. 4, D and E). Similarly, transfection of Gα$_s$ into *GNAS* KO HEK293 cells effectively restored robust ERK signaling (Fig. 4F), supporting the notion that G$_s$ coupling is critical for initiating β$_2$AR-mediated ERK activation.

PKA is dispensable for ERK activation by β$_2$AR

Because protein kinase A (PKA) is a major signaling target of Gα$_s$ and cAMP production, we next tested the role of PKA in β$_2$AR-mediated ERK activation. Similar to previously published results (*11*), we observed that pretreatment with the PKA inhibitor H89 impaired ERK activation by isoproterenol (Fig. 4G). However, H89 is not a very specific inhibitor and can target multiple additional kinases (*19*, *20*). Thus, we tested more selective inhibitors of PKA including the cell-permeable competitive antagonist cAMPS-RP.

In contrast to H89, cAMPS-RP had little effect on isoproterenol-induced ERK activation (Fig. 4H), although it effectively blocked isoproterenol- and forskolin-induced CRE-dependent transcription (Fig. 4I). As a complementary approach, we expressed a GFP-tagged version of protein kinase A inhibitor (PKI), a specific peptide inhibitor of PKA, or control PKI mutant peptide (PKI-Mut), in which the PKA inhibitory domain is disrupted (*21*). The PKI peptide, but not the control PKI-Mut peptide or GFP plasmid alone, disrupted CRE luciferase induction by isoproterenol stimulation (Fig. 4J). However, as with cAMPS-RP, inhibition of PKA with PKI did not impair isoproterenol-induced ERK phosphorylation (Fig. 4J). Because PKA is not the only target of cAMP production downstream of Gα$_s$ activation, we also tested the potential role of EPAC, a RAP1 guanine nucleotide exchange factor, in transmitting signals, leading to ERK activation. However, CE3F4, a small molecule that blocks EPAC-induced RAP1A activation, also failed to reduce isoproterenol-induced ERK activation (fig. S7C), although it successfully disrupted RAP1A activation (fig. S7D).

ERK activation by β$_2$AR is mediated by SRC, SHC, SOS, and RAS

Similar to the absence of direct evidence that PKA is required for β$_2$AR-mediated ERK activation, pharmacological agents inhibiting EGF receptor (EGFR) (AG1478), phosphatidylinositol 3-kinase (PI3K) (LY294002), and Gα$_i$ (pertussis toxin) also failed to prevent ERK activation in response to isoproterenol in HEK293 FLAG-β$_2$AR cells (fig. S8, A to C). Thus, we next decided to delineate signaling upstream of ERK activation after the classic RAS/RAF/MAPK kinase (MEK)/ERK signaling cascade, although, based on our data, it was unlikely that RAF activation could be achieved by a β-arrestin–dependent activation bypassing RAS, as previously proposed (*22*, *23*). The MEK1/2 inhibitor U0126 completely abrogated ERK phosphorylation in response to isoproterenol and EGF (the latter was used as a control), indicating that MEK1/2 was strictly required (Fig. 5A). Working upstream, the B-RAF inhibitors SB-590885 and GDC-0879 similarly abrogated ERK phosphorylation in response to isoproterenol and EGF (Fig. 5B). To evaluate the role of RAS in the activation of ERK, we used dominant-negative KRAS and HRAS plasmids. Transfection of either dominant-negative RAS plasmid reduced the isoproterenol-induced ERK activation, with the KRAS dominant-negative plasma having the more potent inhibitory effect (Fig. 5C). Although expression of dominant negative KRAS substantially disrupted β$_2$AR-mediated ERK phosphorylation, it did not prevent the induction of CRE luciferase by isoproterenol or forskolin, supporting a role for RAS in ERK activation independently of cAMP/PKA-induced Cre transcription (Fig. 5D). Pull-down assays for active Ras indicated that active GTP-bound RAS was increased upon isoproterenol stimulation (Fig. 5E). In a complementary approach, we generated stable FLAG-β$_2$AR–expressing MEFs in which *Hras* and *Nras* genes were deleted and the *Kras* gene was floxed (fig. S8D) (*24*). Stimulation of these "Rasless MEFs," in which treatment with Cre-GFP adenovirus efficiently excised the *Kras* gene, substantially reduced ERK phosphorylation in comparison to adeno-GFP control (Fig. 5F), collectively supporting a key role for RAS in ERK activation by β$_2$AR.

To explore the role of candidate RAS-GEFs involved in activating the RAS/RAF/MEK/ERK signaling cascade, we performed a RAS guanine nucleotide exchange factor (GEF) siRNA library screen, which included siRNAs for each of the eight members of the RAS-GEF superfamily (*25*) and the In-Cell Western blot fluorescence
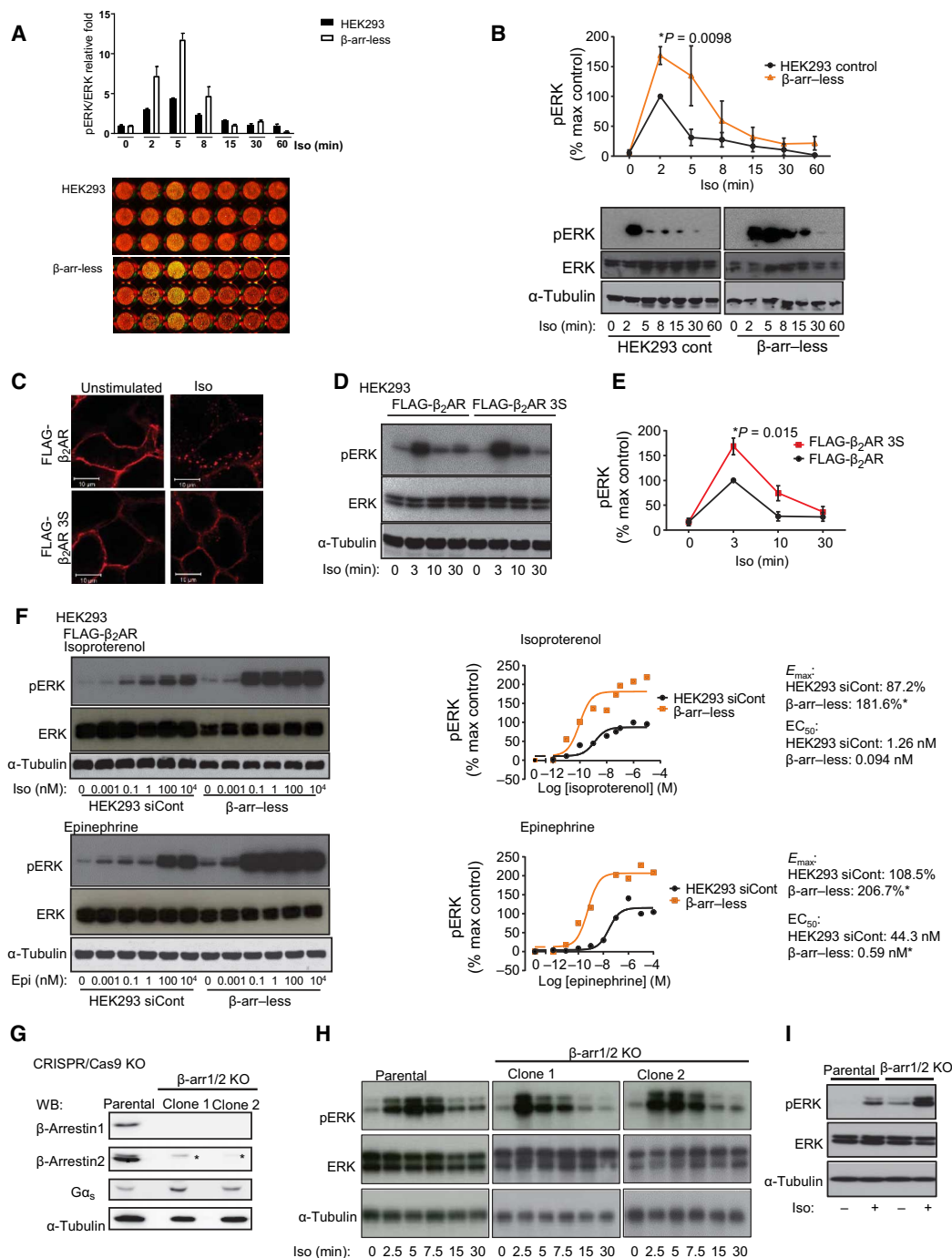
Fig. 3. ERK activation in HEK293 and β-arr–less cells. (**A**) In-Cell Western blot with quantification of ERK phosphorylation (pERK) induced by isoproterenol stimulation, performed in triplicate ± SEM; representative of two independent experiments shown. (**B**) Western blot and quantification of isoproterenol-induced pERK normalized to total ERK from three independent Western blots ± SEM. Statistical significance was determined by t test. Westerns are from the same blot and exposure; representative of three independent experiments. (**C**) Immunofluorescence of FLAG-β₂AR and FLAG-β₂AR 3S in HEK293 cells upon 5-min isoproterenol stimulation. Scale bars, 10 μm. Representative image from two independent experiments. (**D**) Western blot of pERK and indicated controls upon isoproterenol stimulation of HEK293 FLAG-β₂AR or FLAG-β₂AR 3S cells. (**E**) Quantification of pERK normalized to ERK from three independent Western blots ± SEM in the indicated cells after isoproterenol stimulation. Statistical significance was determined by t test. (**F**) pERK Western blots of the indicated cells after 3-min isoproterenol and epinephrine (Epi) stimulations (representative of three independent experiments) and the corresponding representative ELISA data quantifying amounts of pERK (representative of three independent experiments). Relative E_{max} and EC_{50} values are indicated. Nonlinear regression (least squares fit) analysis was used to fit curves and determine the EC_{50} and E_{max} values. Statistical significance (*) signifies nonoverlapping 95% confidence intervals. (**G** and **H**) Western blot for β-arr1 and β-arr2 in parental HEK293 cells and two separate CRISPR/Cas9 β-arr1/2 KO clones (asterisks in the β-arrestin 2 panel indicate nonspecific immunoreactive bands) (G) and pERK amounts upon isoproterenol stimulation of these cells (H). Representative of three independent experiments. (**I**) Western blot for pERK, total ERK, and α-tubulin in unstimulated and 5-min isoproterenol (10 μM) stimulated parental HEK293 and β-arr1/2 KO cell lines with endogenous levels of β₂AR. Results represent three independent experiments.
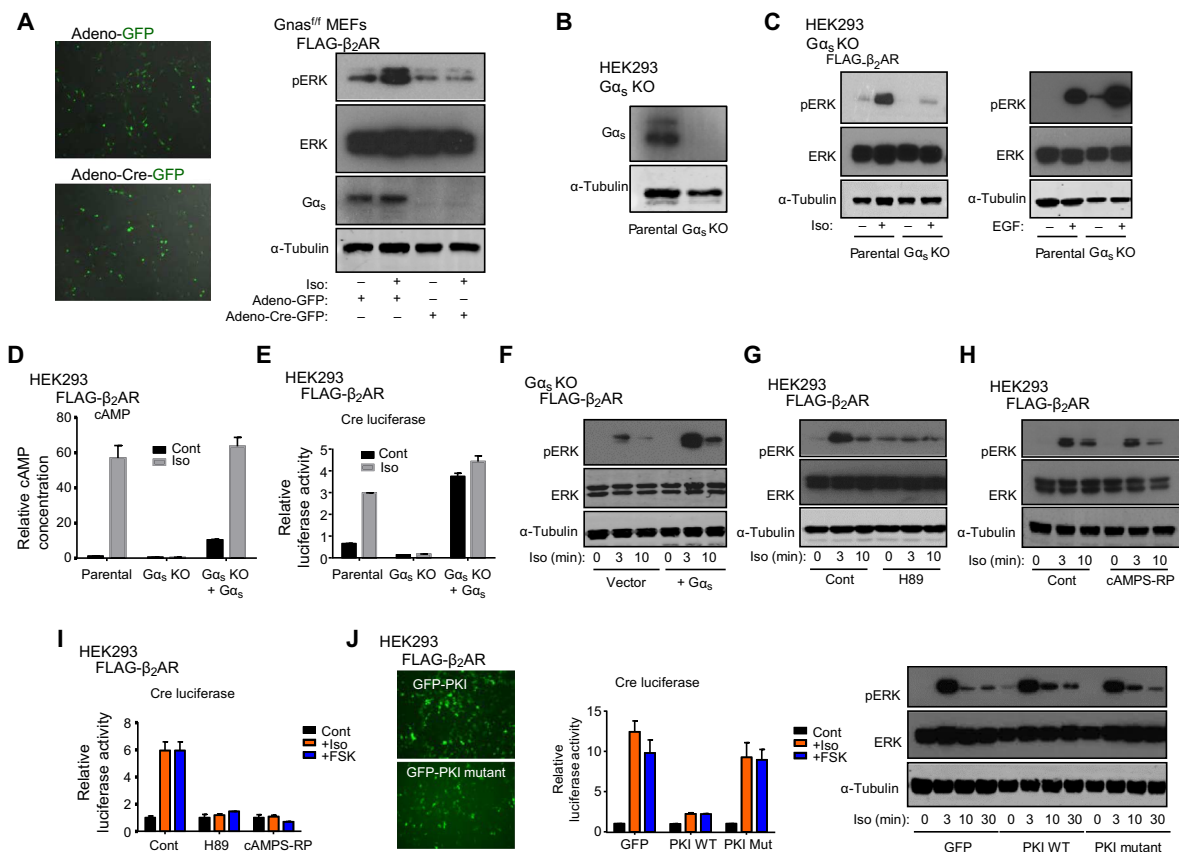
Fig. 4. Gα$_s$, but not PKA, is critical for β$_2$AR-mediated ERK phosphorylation. (**A**) Immunofluorescence showing GFP expression of FLAG-β$_2$AR *Gnas* f/f MEFs transduced with control adenoviral (adeno)–GFP or adeno-Cre-GFP and Western blot of pERK upon 3-min isoproterenol stimulation of these cells (representative of three independent experiments). (**B**) Western blot for Gα$_s$ in HEK293 CRISPR/Cas9-edited Gα$_s$ KO cells. (**C**) Western blot of pERK upon 3-min isoproterenol or EGF (10 ng/ml) stimulation in the indicated cells. Representative of three independent experiments. (**D** and **E**) Relative amounts (mean ± SEM of three independent experiments) of cAMP (D) and CRE luciferase activity (E) in the indicated cells upon isoproterenol stimulation. (**F**) Western blot of pERK after isoproterenol stimulation in Gα$_s$ KO FLAG-β$_2$AR cells transfected with vector control or Gα$_s$. Representative of three independent experiments. (**G** and **H**) Western blot of pERK in HEK293 FLAG-β$_2$AR cells stimulated with isoproterenol after pretreatment with dimethyl sulfoxide (DMSO) (control), H89 (10 μM) (G), or cAMPS-RP (100 μM) (H). Representative of three independent experiments for (G) and (H). (**I**) Relative CRE luciferase activity in isoproterenol- and forskolin (FSK; 5 mg/ml)–stimulated HEK293 FLAG-β$_2$AR cells pretreated with H89, cAMPS-RP, or DMSO control; mean ± SEM of three experiments. (**J**) Immunofluorescence of GFP expression, relative CRE luciferase activity (mean ± SEM, three experiments), and Western blot of pERK in HEK293 FLAG-β$_2$AR cells transfected with GFP-PKI or GFP-PKI-mutant (PKI-Mut) plasmids upon stimulation with isoproterenol (representative of three independent experiments).

assay described above. Among the GEFs tested, SOS1 and SOS2 had the most significant *z* scores, therefore representing the best candidates for mediating isoproterenol-induced ERK phosphorylation in β$_2$AR-expressing HEK293 cells (Fig. 5G). We confirmed a critical role for SOS1 and SOS2 in β$_2$AR-mediated ERK activation by Western blot analysis of cells transfected with a pool of siRNAs targeting SOS1 and SOS2 (Fig. 5H). Because SHC and upstream SRC family kinases can activate SOS-RAS signaling, we investigated whether β$_2$AR stimulation mediated phosphorylation of SRC and SHC. Isoproterenol stimulation caused an increase in tyrosine phosphorylation of SHC and SRC (Y416) (Fig. 5I). Additionally, the small-molecule SRC inhibitors SU6656 and PP1 impaired the isoproterenol-induced phosphorylation of SRC and SHC (Fig. 5J) and substantially reduced ERK activation (Fig. 5K). Cells depleted of β-arrestins (β-arr–less cells) showed largely normal isoproterenol-induced phosphorylation of SRC (Fig. 5L). Therefore, SRC appears to play an important role in β$_2$AR-mediated ERK activation that is independent of β-arrestins. Finally, we examined whether Gβγ sig-

naling upon Gα$_s$ activation may be important for ERK activation. An HA-tagged C-terminal GRK2 construct (HA-GRK2ct), which selectively blocks βγ signaling (also known as βARKct) (26), substantially reduced the β$_2$AR-mediated ERK phosphorylation without affecting EGF-mediated ERK activation (Fig. 5M). Additionally, inhibition of βγ signaling through GRK2ct also significantly disrupted the phosphorylation of SRC and SHC (Fig. 5N and fig. S8E). Thus, Gβγ signaling appears to play a key role in the initiation of a signaling cascade involving SRC, SHC, SOS, RAS, RAF, MEK, and ERK that links β$_2$AR to ERK (Fig. 6).

DISCUSSION
The scaffolding and proposed activation of ERK by β-arrestins has received considerable attention due to the critical role of ERK in cell growth, survival, and proliferation responses. Additionally, ERK activation is frequently monitored in high-throughput drug screens for "biased" GPCR agonists and antagonists, in which G
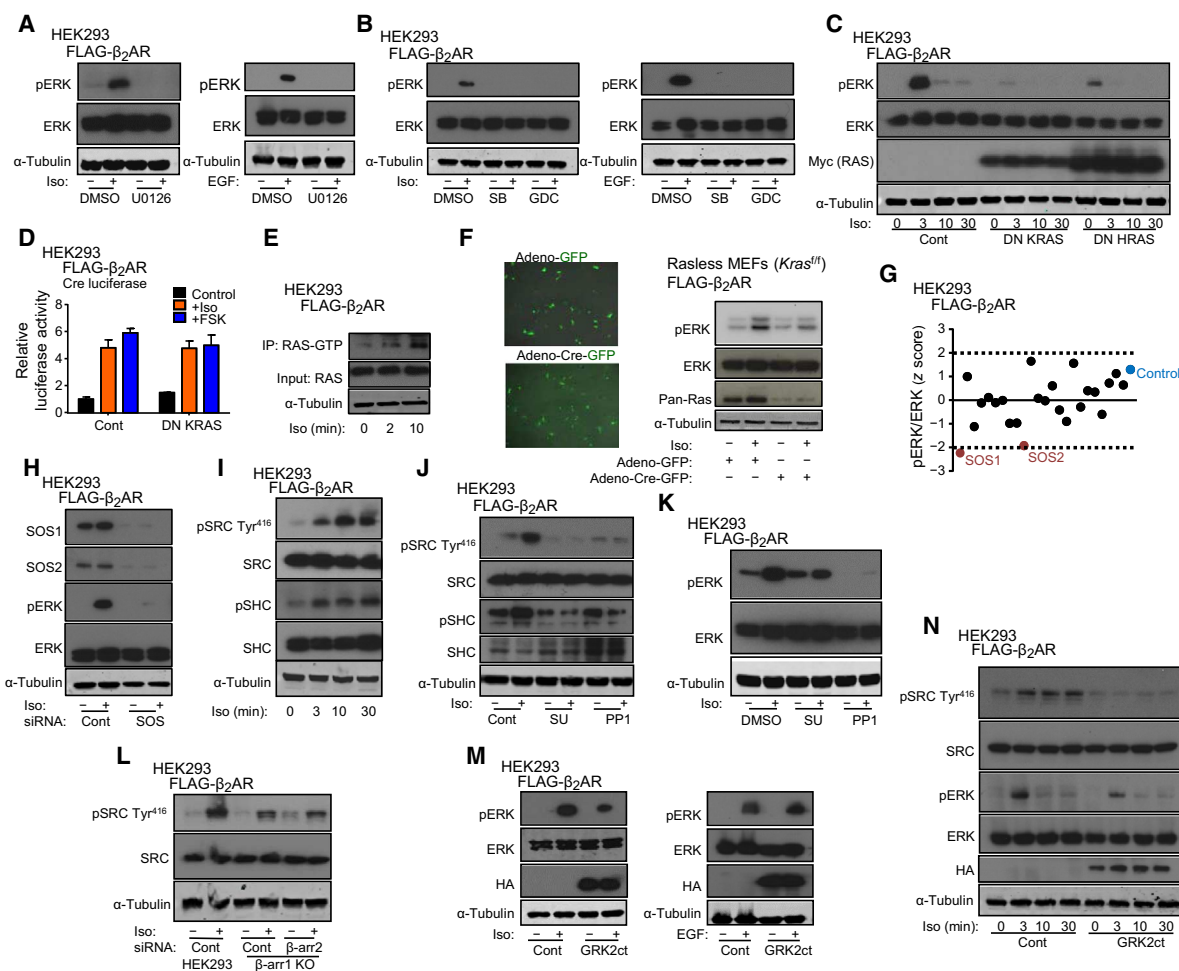
Fig. 5. β₂AR-mediates ERK activation through Gβγ signaling and activation of a signaling cascade that involves SRC, SHC, SOS, RAS, RAF, and MEK. (**A** and **B**) Western blot of pERK after isoproterenol or EGF stimulation (3 min) in HEK293 FLAG-β₂AR cells pretreated with DMSO or U0126 (10 μM) (A), SB-590885 (SB; 10 μM) (B), or GDC-0879 (GDC; 10 μM) (B). Representative of three independent experiments for (A) and (B). (**C**) Western blot of pERK after isoproterenol stimulation in HEK293 FLAG-β₂AR cells transfected with dominant-negative (DN) KRAS, dominant-negative HRAS, or control. Representative of four independent experiments. (**D**) Relative CRE luciferase activity in isoproterenol- and forskolin-stimulated HEK293 FLAG-β₂AR cells transfected with dominant-negative KRAS or control plasmid; mean ± SEM of three experiments. (**E**) Western blot showing active RAS-GTP pull-down (IP) and input for RAS and α-tubulin after isoproterenol stimulation. Representative of three independent experiments. (**F**) Immunofluorescence showing GFP expression and pERK Western blot of isoproterenol-stimulated FLAG-β₂AR–Rasless MEFs transduced with adeno-GFP or adeno-Cre-GFP virus (representative of three independent experiments). (**G**) Effects of an siRNA library screen of various RAS–guanine nucleotide exchange factors (GEFs) on isoproterenol-stimulated pERK amounts. Representative of three independent experiments. (**H**) Western blot of pERK in HEK293 FLAG-β₂AR cells transfected with siRNA to SOS1 and SOS2 (SOS) or control in response to isoproterenol. Representative of three independent experiments. (**I** and **J**) Western blot of pSRC and pSHC in (I) response to isoproterenol stimulation and (J) with the SRC inhibitor PP1 (10 μM), SU6656 (SU; 10 μM), or DMSO. Representative of three independent experiments for (I) and (J). (**K**) Western blot of pERK in HEK293 FLAG-β₂AR cells pretreated with SRC inhibitors upon isoproterenol stimulation. Representative of three independent experiments. (**L**) Western blot of pSRC in the indicated cells upon isoproterenol stimulation. Representative of three independent experiments. (**M**) Western blot of pERK after isoproterenol or EGF stimulation in HEK293 FLAG-β₂AR cells transfected with control or hemagglutinin (HA)–tagged GRK2ct plasmids. Representative of three independent experiments. (**N**) Western blot of isoproterenol-stimulated pSRC and pERK in HEK293 FLAG-β₂AR cells transfected with control or HA-tagged GRK2ct. Representative of three independent experiments.

protein signaling may be inhibited, whereas β-arrestin function is maintained, and vice versa. Although β-arrestins have been proposed to interact with and induce their own G protein–independent activation of ERK (9, 27), our results showed that loss of β-arrestins enhanced the potency and efficacy of isoproterenol- and epinephrine-induced ERK phosphorylation. Therefore, it is possible that the effects of β-arrestins on desensitization of G protein signaling, including G protein–dependent ERK activation, override their potential direct contributions to ERK activation. Hence, not only cAMP signaling but

also ERK phosphorylation responses are enhanced in β-arrestin–depleted and KO cells.

Overall, the combination of genome editing approaches with siRNA-mediated knockdowns, conditional gene deletion in engineered fibroblasts, and genome editing cell KOs for critical signaling nodes provided genetic evidence supporting that β-arrestins play distinct roles in β₂AR internalization and desensitization, including a preferential role for β-arr2 in β₂AR internalization (4, 5, 8, 28), while revealing that β-arrestins are dispensable for ERK activation and
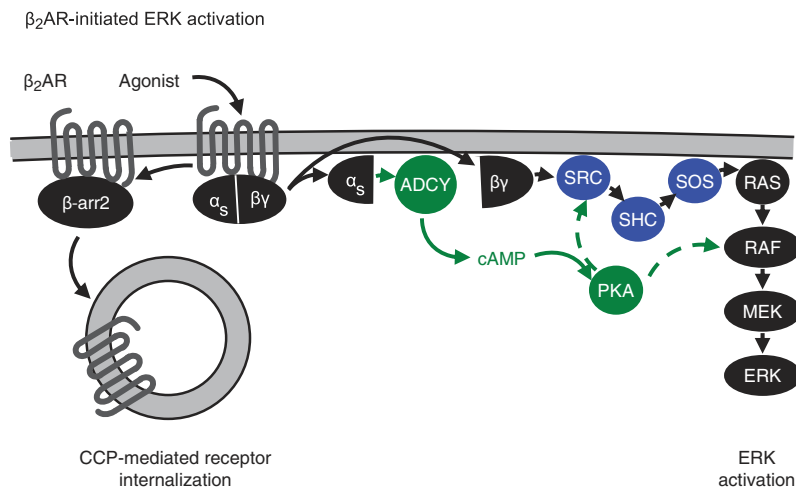
Fig. 6. Schematic depicting β2AR-mediated ERK activation. β2AR-mediated ERK activation occurs through Gβγ induction of a signaling cascade that involves SRC, SHC, SOS, RAS, RAF, and MEK. β-arr2 mediates endocytosis of β2AR through clathrin-coated pits (CCPs), and Gα activates adenylate cyclase (ADCY) to generate cAMP, thereby activating PKA. Although PKA is dispensable for the activation of the SRC/SHC/SOS/RAS/RAF/MEK/ERK pathway by β2AR, it will require further investigation to determine whether PKA redundantly feeds into this pathway.

function. Specifically, our findings are consistent with a model in which β2AR stimulation promotes the activation of Gαs, promoting the accumulation of cAMP through Gαs and ERK activation primarily through Gβγ subunits (Fig. 6). In the absence of Gβγ signaling, the limited residual ERK activation may suggest the existence of additional minor contributing mechanisms that may require further elucidation, such as a cAMP-dependent activation that is not strictly necessary for β2AR activation of ERK (Fig. 6). In turn, Gβγ may stimulate the kinase activity of SRC directly, as has been previously demonstrated using in vitro reconstitution systems and purified components (29, 30), and the sequential activation of RAS and the ERK kinase cascade through SOS1/2 upon SHC phosphorylation by SRC (Fig. 6). Overall, our results support that initiation of ERK activation by β2AR involves a signaling route that is independent of β-arrestins, with β-arrestins inhibiting rather than activating ERK in this pathway.

These findings may have general implications for signaling to ERK through Gαs-coupled GPCRs. Specifically, β2AR is a prototypical GPCR that associates transiently with β-arrestins, often referred to as class A GPCR, as compared to class B GPCRs, which include AT1A angiotensin receptors and V2R vasopressin receptors and associate tightly with β-arrestins and are co-internalized (31). The use of β-arrestin KO cells suggests that, at least for V2R, β-arrestins are not strictly required for ERK signaling by this class B GPCR. ERK phosphorylation downstream of activation of the free fatty acid receptor 4 (FFA4), which couples with Gαq, depends on Gαq but not β-arrestins (32). Thus, the dispensable role of β-arrestin in GPCR-induced ERK activation is likely to be generalizable and is supported by several additional studies (33, 34). On the other hand, the role of receptor internalization for prolonged ERK activation by class B GPCRs has been traditionally interpreted as β-arrestin–initiated ERK signaling (9). However, class B GPCRs form a ternary complex, with β-arrestins binding to the C-terminal phosphorylated tail of the GPCR and Gαs remaining bound to the receptor, likely locked in a signaling-competent conformation (35). This observation may help explain the fact that many GPCRs can promote long-lasting accumulation of cAMP from an intracellular compartment, including early endosomes (36), through Gαs that is co-internalized with the GPCRs and β-arrestins (37). Thus,

our current study raises the possibility that ERK signaling by class B GPCRs may also involve Gαs rather than a β-arrestin–initiated process once internalized. In this scenario, Gβγ subunits released from Gαs in the proximity of β-arrestin–bound GPCR-Gαs complexes may promote the persistent activation of SRC, RAS, and ERK from an intracellular compartment. The activation of RAS, particularly that of KRAS in an intracellular membrane compartment, has been reported, which may have distinct signaling output in terms of amplitude and duration and biological activity (38). In this context, previous observations that β-arrestins bind ERK and its upstream components could be reinterpreted as a reflection of the scaffolding function of β-arrestins, which may control the localized activation of ERK rather than promote ERK activation. However, we note that β-arr2 knockdown reduces ERK activation by the β1AR (39), opposite to its effect on ERK activation by β2AR. Thus, it is possible that functional diversity between receptors is achieved through receptor-specific differences in the degree to which ERK activation is limited by β-arrestins' distinct signal-attenuating and scaffolding functions. Cell type–specific differences in signaling specificity may also come into play, and so, future studies using new genome editing approaches may help clarify these issues in specific cell populations.

The use of genome editing strategies and targeted gene deletion in MEFs provide enormous power for improving knowledge of GPCR and β-arrestin function by the genetic dissection of receptor-specific differences in signaling, desensitization, and trafficking. Overall, we could link β-arrestins to desensitization of β2AR-mediated signaling and identify a selective function for β-arr2 in endocytosis of β2AR mediated by clathrin-coated pits. Analysis of ERK activation also revealed the need for caution when using ERK as a screen for β-arrestin–biased agonists and for considering β-arrestins in overall ERK signaling and function because we observed a critical role for Gαs signaling and a desensitizing role of β-arrestins in the overall ERK activation. Thus, the use of genome-edited cellular systems to screen for biased drug responsiveness may provide better insights into the mechanisms by which they exert their pharmacological effects. Overall, we have defined a molecular framework by which β2AR initiates ERK activation by a β-arrestin–independent pathway. Ultimately, our findings provide a mechanism by which multiple GPCRs may control ERK-regulated gene transcription programs and the consequent orchestration of cell-specific biological responses that are dependent on ERK.

MATERIALS AND METHODS
Reagents
Isoproterenol, forskolin, EGF, epinephrine, thrombin, U0126, PP1, SU6656, and H89 were purchased from Sigma. 8-(4-Chlorophenylthio)adenosine-3′,5′-cyclic monophosphate (8-CPT-cAMP) and 8-(4-chlorophenylthio)-2′-O-methyl-cAMP (8-pCPT-2′-O-Me-cAMP) were from BIOLOG Life Science Institute (Axxora). CE3F4, cAMPS-RP, SB-590885, and GDC-0879 were obtained from Tocris. Pertussis

toxin (PTX) was obtained from List Biological Laboratories Inc. AG1478 and LY294002 were obtained from Calbiochem. siRNAs targeting β-arr1, β-arr2, clathrin heavy chain (CHC-17), and AllStars Negative Control were purchased from Qiagen. Sandwich ELISA kit for phopsho-ERK1/2 and antibodies against phospho-ERK1/2 [phospho-p42/p44 MAPK (Thr[202]/Tyr[204]) XP], ERK1/2 (p42/44 MAPK), β-arr1, β-arr2, β-arr1/2, phospho-Akt (Ser[473]) (D9E) XP, Akt, phospho-SRC (Tyr[416]), SRC (32G6), phospho-SHC (Tyr[239/240]), and α-tubulin (DM1A) were from Cell Signaling Technology. Gα$_s$, SOS1, and SOS2 antibodies were obtained from Santa Cruz Biotechnology. SHC antibody was from Millipore/Upstate Biotechnology. Pan-RAS (Ab-3) antibody was from Calbiochem. Antibodies against HA and Myc (9E10) tags were obtained from Covance. FLAG–phycoerythrin (PE) antibody (PJ315) was from Prozyme. EEA1 and clathrin heavy chain antibodies were purchased from BD Biosciences. Secondary horseradish peroxidase–conjugated antibodies were purchased from GE Healthcare, and Alexa Fluor 680– and Alexa Fluor 800–conjugated secondary antibodies for LI-COR imaging were from Invitrogen. SNAP surface Alexa Fluor 488 and 546 labels were purchased from New England Biolabs. Puromycin, transferrin–Alexa Fluor 546, Alexa Fluor 546, and Alexa Fluor 488 were purchased from Invitrogen. Prepackaged adenoviruses, adeno-GFP and adeno-GFP iCre, were obtained from Vector Biolabs.

Plasmids and constructs

FLAG-β$_2$AR was expressed in pcDNA3.1 vector for transient transfections or subcloned into our in-house pLESIP lentiviral expression vector for stable transductions. FLAG-β$_2$AR 3S (S355G, S356G, and S364G) mutant was prepared as previously described (37). The SNAP-β$_2$AR plasmid used for imaging studies was purchased from New England Biolabs. Gα transducin and myc-tagged dominant-negative RAS mutants (KRAS S17N and HRAS S17N) were purchased from Missouri S&T cDNA Resource Center. PKI and PKI mutant plasmids were prepared as previously described (21). Clathrin light chain–dsRed used for TIRF microscopy was previously described (40). pCDNA3.1$^+$ HA-AVP2R DNA was purchased from cDNA Resource Center (Bloomsburg University, Bloomsburg, PA). The HA-tagged GRK2ct was prepared performing polymerase chain reaction (PCR) on GRK2 amino acid residues 495 to 689, with the addition of an N-terminal HA tag, and inserted into our in-house pCEFL vector. Construct sequence was verified by DNA sequence analysis (National Institute of Dental and Craniofacial Research shared resource facility). Human GNAS open reading frame (short isoform) was PCR-amplified from reverse-transcribed human total mRNA (FirstChoice Human Total RNA Survey Panel, Ambion) and cloned into a pCAGGS expression vector (a gift from J.-i. Miyazaki, Osaka University, Japan). The inserted fragment was sequenced with the Sanger sequencing method (Fasmac).

Cell culture

HEK293, Rasless MEFs, and Gnas f/f MEFs were cultured in Dulbecco's modified Eagle's medium (DMEM) (Sigma) supplemented with 10% fetal bovine serum (FBS) (Sigma) and penicillin/streptomycin (Sigma). Rasless MEFs were derived from Nras and Hras KO mice harboring a floxed allele of Kras as previously described (24). Gnas f/f MEFs were provided by J. Regard and generated as previously described (41). Gα$_s$ KO HEK293 cells were prepared using CRISPR/Cas9 as previously reported (42).

Generation of the β-arr1 TALEN KO HEK293 cell line

The Cornell TALEN Targeter software was used to identify β-arr1 TALEN sites and check for potential off-target sites (https://tale-nt.

cac.cornell.edu/). The β-arr1 TALEN was designed to target the following sequence corresponding to a region of exon 6, in which capital letters correspond to TALEN binding sites and the lowercase letters correspond to the spacer region sequence: TCCCTCCAAAC-CTTCCATGTtctgtgacactgcagccgGGGCCCGAAGACACGGGGAA. TALENs were assembled using the EZ-TAL Assembly Kit (System Biosciences), and the repeat-variable diresidue (RVD) sequences of the assembled β-arr1 TALENs were as follows: TAL1 RVD, HD HD HD NG HD HD NI NI NI HD HD NG NG HD HD NI NG NH NG; TAL2 RVD, NG HD HD HD HD NH NG NH NG HD NG NG HD NH NH NH HD HD HD. A surveyor nuclease assay was performed to confirm targeting of the TALEN at the appropriate β-arr1 locus. Briefly, genomic DNA was isolated using the QIAamp DNA Isolation Kit (Qiagen) and amplified with the AccuPrime SuperMix (Life Technologies) using oligos surrounding the TALEN cut site (forward primer: GTTCAAGAAGGCCAGTCCAAATGGAAAGC; reverse primer: CTGATGGGTTCTCCATGGTAATAGATCTCC). A surveyor nuclease assay was then performed on PCR-amplified DNA from control- or TALEN-transfected HEK293 cells using the Surveyor Mutation Detection Kit (Transgenomic Inc.). To generate the β-arr1 TALEN KO (β-arr1 KO) cell line, HEK293 cells were transfected using TurboFect transfection reagent (Fermentas) and clonally selected by limited dilution. Single-cell clones were expanded and then screened by surveyor nuclease assay and Western blot for loss of β-arr1.

Generation of the β-arr1/2 CRISPR double-KO HEK293 cell line

The β-arr1/2 CRISPR KO HEK293 cell line was generated by simultaneously targeting the ARRB1 and the ARRB2 genes using a CRISPR/Cas9 system as described previously (14, 43) with minor modifications. Designed single-guide RNA (sgRNA)–targeting sequences in the ARRB1 gene were 5′-TTCCCCGTGTCTTCGGGCCC**CGG**-3′ [ARRB1 target #1; the SpCas9 PAM sequence (NGG) is in bold letters and the Apa I recognition site is underlined; note that the sgRNA-targeting sequences are complement to the direction of the ARRB1 transcription] and 5′-CGCCTTCCGCTATGGCCGGG**AGG**-3′ (ARRB1 target #2; Hap II is underlined). The ARRB1 sgRNA-targeting sequences were inserted into the Bbs I site of the pSpCas9(BB)-2A-GFP (PX458) vector (a gift from F. Zhang, Broad Institute; Addgene plasmid #42230) using two sets of synthesized oligonucleotides [5′-CACCGTTCCCCGT-GTCTTCGGGCCC-3′ and 5′-AAACGGGCCCGAAGACACGGG-GAAC-3′, and 5′-CACCGCGCCTTCCGCTATGGCCGGG-3′ and 5′-AAACCCCGGCCATAGCGGAAGGCGC-3′, respectively; custom-synthesized by Fasmac; note that a guanine nucleotide (G) was introduced at the −21 position of the sgRNA (underlined), which enhances transcription of the sgRNA]. Similarly, sgRNA-targeting sequences in the ARRB2 gene were 5′-CCAAAAGCTGTACTACCATG**GGG**-3′ (ARRB2 target #1; the PAM sequence is in bold letters and the Nco I recognition site is underlined) and 5′-TGACCGGTCCCTGCACCTC-G**AGG**-3′ (ARRB2 target #2; Xho I recognition site is underlined) and were inserted using a pair of oligonucleotides (5′-CACCGCCAAA-AGCTGTACTACCATG-3′ and 5′-AAACCATGGTAGTACAGC-TTTTGGC-3′, 5′-CACCGTGACCGGTCCCTGCACCTCG-3′ and 5′-AAACCGAGGTGCAGGGACCGGTCAC-3′, respectively). Correctly inserted sgRNA-encoding sequences were verified by sequencing using the Sanger method (Fasmac).

HEK293A cells (Thermo Fisher Scientific) were seeded into a 12-well plate (50,000 cells per well in 1 ml of medium) and incubated for 24 hours before transfection. A mixture of the ARRB1-targeting

vector (0.25 μg) and the *ARRB2*-targeting vector (0.25 μg) was transfected into the cells using 1.25 μl of Lipofectamine 2000 (Life Technologies). After a 3-day incubation, the cells were harvested with trypsin/EDTA, and GFP-positive cells were isolated using an SH800 cell sorter (Sony). The GFP-positive cells were diluted with DMEM supplemented with 10% FBS and penicillin/streptomycin and seeded in 96-well plates to isolate single clones using a limiting dilution method. The seeded 96-well plates were incubated for about 2 weeks with routine addition of fresh medium and observed under microscope for their colony appearances. While passaging clonal cells into a six-well plate, an aliquot of cell suspensions was analyzed for mutations in the targeted sites using PCR and restriction enzyme digestion. For mutational analysis of the *ARRB1* target #1, PCR was performed using primers 5′-TTAGATGGGGCATGGCTTGG-3′ and 5′-GAGTGGTCCTGT-GTGTCCAG-3′), and the PCR amplicon was digested with Apa I (Takara Bio). Similarly, the following primers and restriction enzymes were used: for the *ARRB1* target #2, primers 5′-GGCATCCTTCCGG-TACTCAC-3′ and 5′-GTCAGGGGCTTCTTGTCCTC-3′ and Hap II; for the *ARRB2* target #1, primers 5′-ACGGTGCAGTTTAGACCCTG-3′ and 5′-TGACGGTCTTGGTGGAGTTG-3′ and Nco I; for the *ARRB2* target #2, primers 5′-TCCTGCCCCTACTCTGATCC-3′ and 5′-CCCCAGGGTCTAAACTGCAC-3′ and Xho I. A PCR program started with an initial denaturation cycle of 95°C for 2 min, followed by 35 cycles of 95°C for 15 s, 64°C for 30 s, and 72°C for 30 s. The resulting PCR product (5 μl) was digested with a corresponding restriction enzyme (0.5 μl) in a reaction buffer (total volume of 10 μl) and incubated at 37°C for 1 hour. Digested DNA fragments were analyzed with the MultiNA Microchip Electrophoresis System (Shimadzu). Candidate clones that harbored restriction enzyme–resistant PCR fragments were further assessed for their genomic DNA alterations by TA cloning. Lack of functional β-arrestins was also confirmed by assessing protein expression and ligand-stimulated GPCR internalization as described below. For the TA cloning, PCR-amplified genomic DNA fragments using an Ex Taq polymerase (Takara Bio) were gel-purified (Promega) and cloned into a pMD20 T-vector (Takara Bio). Ligated products were introduced into SCS1 competent cells (Stratagene), and transformed cells were selected on an ampicillin-containing LB plate. At least 12 colonies were picked, and inserted fragments were PCR-amplified using the Ex Taq polymerase and primers [5′-CAG-GAAACAGCTATGAC-3′ (M13 Primer RV) and 5′-GTTTTCCCAG-TCACGAC-3′ (M13 Primer M4)] designed to anneal the pME20 T-vectors. PCR products of the transformed pMD20 T-vector were sequenced using the Sanger method (Fasmac) and the M13 Primer RV.

Transfection, RNA interference, and viral transduction

Transient transfections of plasmid DNAs were performed using Lipofectamine 2000 (Invitrogen) reagent for 48 hours. Transfections of siRNAs were performed using Lipofectamine RNAiMAX (Invitrogen) using 50 nM siRNAs for 72 hours to achieve RNA interference–mediated knockdown. Cells transfected with both siRNA and plasmid DNA were first transfected with siRNA for 24 hours, followed by a medium change before transfection with plasmid DNA for another 48 hours.

FLAG-β₂AR and FLAG-β₂AR 3S lentiviruses were prepared by transfecting HEK293T/17 cells (ATCC CRL-11268) with pLESIP FLAG-β₂AR, psPAX2, and vesicular stomatitis virus glycoprotein in a 3:2:1 ratio using TurboFect transfection reagent (Fermentas) and collecting 48- and 72-hour viral supernatants. HEK293, β-arr1 KO cells, Rasless MEFs, and *Gnas* f/f MEFs were transduced by infection with 0.45 μm polyvinylidene difluoride (PVDF)–filtered FLAG-β₂AR lentivi-

rus with polybrene (6 μg/ml) and then selected with puromycin (1 μg/ml) (Invitrogen) to generate stable lines. Expression of FLAG-β₂AR was verified by flow cytometry using a FLAG-PE–conjugated antibody (Prozyme) and analyzed on a FACSCalibur (BD Biosciences). Adenoviral transductions of Rasless MEFs and *Gnas* f/f MEFs with adeno-GFP control or adeno-GFP iCre to delete *Kras* or *Gnas* (Gα_s), respectively, involved infection of cells with 2.8×10^7 plaque-forming units/ml of virus plus polybrene (6 μg/ml) for 72 hours. Infection was confirmed by fluorescence microscopy for GFP expression and Western blot analysis for loss of Ras or Gα_s in the Cre-infected MEFs.

Internalization assays

Internalization assays were performed by FLAG-PE surface staining of stably transduced FLAG-β₂AR HEK293 and β-arr1 KO cells before and after specified time points of stimulation with 10 μM isoproterenol. As indicated, cells were transfected with appropriate siRNAs for 72 hours before internalization assay. After stimulation, cells were incubated on ice and quickly rinsed with ice-cold phosphate-buffered saline (PBS). Cells were lifted with 1 mM EDTA in PBS, centrifuged at 3000 rpm for 5 min at 4°C, and stained in a 100-μl volume of 0.5% bovine serum albumin (BSA)–PBS with 1.25 μl of FLAG-PE (Prozyme) antibody covered on ice. Cells were washed three times with 1 ml of cold 0.5% BSA-PBS and then analyzed on a FACSCalibur (BD Biosciences). Transferrin internalization assays were performed by incubating cells in serum-free DMEM with or without conjugated transferrin–Alexa Fluor 546 (Invitrogen) for 15 min followed by washes with DMEM and PBS and resuspension in 0.5% BSA-PBS for flow cytometry. Flow cytometry data analysis and MFI values were calculated by FlowJo analysis software on live-gated cells. Percent internalization was calculated based on MFI values as follows: % internalization = $(1 - \text{MFI time point/MFI unstimulated}) \times 100$.

Cre luciferase assay

Cre luciferase assays were performed by seeding HEK293 stably transduced with FLAG-β₂AR cells in a poly-lysine–coated 24-well plate and culturing in DMEM supplemented with 10% FBS for 24 hours. Cells were then cotransfected with 100 ng of plasmid DNA or control, 50 ng of Cre-firefly luciferase reporter DNA, and 20 ng of pRL-*Renilla* luciferase using Lipofectamine 2000 (Life Technologies) transfection reagent. The day after transfection, cells were serum-starved, treated with appropriate inhibitors when relevant, and then stimulated for 6 hours with isoproterenol (10 μM) before harvesting the cells. For all Cre-luciferase assays, cells were lysed and luciferase activity was determined using the Dual-Glo Luciferase Assay Kit (Promega). Chemiluminescence was measured using a BioTek Synergy Neo plate reader, and Cre activation was calculated as the ratio of firefly to *Renilla* luciferase levels. The assays were performed three times in duplicate.

Confocal microscopy

Confocal immunofluorescence and live cell images were collected on a Zeiss LSM 700 laser scanning microscope with a 40× oil immersion lens in a multitrack mode using dual excitation (488 nm for Alexa Fluor 488 and 555 nm for mRFP) and emission (band-pass, 505 to 530 for Alexa Fluor 488; long-pass, 560 nm for mRFP) filter sets. For experiments examining SNAP-β₂AR trafficking, HEK293 and β-arr1 KO cells transfected with SNAP-β₂AR and siRNAs as specified were seeded in poly-lysine–coated 35-mm glass-bottomed culture dishes for live cell (MatTek Corporation) or 1-mm coated glass

coverslips (Fisher) in a six-well plate for fixed immunofluorescence imaging. Cells were labeled with appropriate SNAP surface Alexa Fluor dyes for 30 min at 37°C and then washed three times with complete medium before imaging. Cells for immunofluorescence imaging were stimulated for indicated times with isoproterenol and then washed with PBS and fixed with 2% formaldehyde/PBS solution for 12 min. Fixed cells were blocked in 10% FBS/PBS and then permeabilized with 0.05% saponin (Sigma) solution and incubated with EEA1 (BD Biosciences) antibody for 1 hour at room temperature. Coverslips were washed three times for 5 min with 10% FBS/PBS and then stained with anti-mouse Alexa Fluor 546 antibody for 1 hour at room temperature. Coverslips were washed again and then mounted onto glass slides (Fisher) with FluorSave (Calbiochem) mounting solution.

Live-cell TIRF microscopy imaging

TIRF microscopy was performed at 37°C using a Nikon Ti-E inverted microscope equipped for through-the-objective TIRF microscopy and outfitted with a temperature-, humidity-, and CO$_2$-controlled chamber (Okolab). Images were obtained with an Apo TIRF 100×, 1.49–numerical aperture objective (Nikon) with solid-state lasers of 488, 561, and 647 nm (Keysight Technologies) as light sources. An iXon DU+ DU-897 Andor camera controlled by NIS-Elements 4.1 software was used to acquire image sequences every 2 s for 10 min. HEK293 cells were transfected with the appropriate Alexa Fluor 647–labeled siRNAs for 24 hours, followed by a medium change before transfection with FLAG-β$_2$AR and clathrin light chain–dsRed for 48 hours. Cells were plated on poly-L-lysine (Sigma)–coated 35-mm glass-bottomed culture dishes (MatTek Corporation). Before imaging, cells were labeled 1:1000 with M1 FLAG antibody conjugated to Alexa Fluor 488 dye for 10 min at 37°C, washed, and imaged live in DMEM without phenol red [University of California, San Francisco (UCSF) Cell Culture Facility] supplemented with 30 mM Hepes (pH 7.4) (UCSF Cell Culture Facility). Cells were stimulated with bath application of 10 μM isoproterenol at frame 10 of 301 image sequences.

TIRF microscopy image analysis

Acquired image sequences were saved as stacks of 16-bit TIFF files. All quantitative image analysis was performed on unprocessed images using ImageJ software (http://rsb.info.nih.gov/ij, U.S. National Institutes of Health). To quantify change in receptor fluorescence over time, fluorescence values of individual cells were measured in five randomly selected regions of interest (ROIs) in the cell over the entire stack. An area of the coverslip-lacking cells was used to estimate background fluorescence. Fluorescence values of the five ROIs were background-subtracted, averaged, normalized to initial fluorescence values before agonist addition, and then normalized to photobleaching control images. Minimal bleed-through and photobleaching was verified using single-labeled and untreated samples, respectively. To quantify receptor concentration into clathrin-coated pits, a line selection was drawn through several clathrin light chain–dsRed foci, representing clathrin-coated pits, at the indicated time points. The plot profile function was used to measure pixel values along this line in the clathrin light chain–dsRed and FLAG-β$_2$AR channels. Pixel values were then normalized and represented as a percent of maximum fluorescence for each channel.

Western blot and pERK ELISA

For cell stimulations for Western blot, HEK293 and β-arr1 KO cells transfected with siRNAs and Rasless MEFs and *Gnas* f/f cells treated for 72 hours with adeno-iCre or adeno-GFP control were left untreated or treated with 10 μM isoproterenol at indicated time points. Additional 3-min stimulations with forskolin (5 mg/ml) or EGF (10 ng/ml) were also performed when indicated. For the experiments done with pharmacological inhibitors, confluent cells were first treated with the vehicle control (DMSO), LY294002 (25 μM) for 1 hour, AG1478 (10 μM) for 1 hour, U0126 (10 μM) for 90 min, PP1 (10 μM) for 1 hour, SU6656 (10 μM) for 1 hour, H89 (10 μM) for 1 hour, CE3F4 (10 μM) for 1 hour, cAMPS-RP (100 μM) for 30 min, SB-590885 (10 μM) for 4 hours, GDC-0879 (10 μM) for 4 hours, or PTX (50 ng/ml) for 16 hours before isoproterenol stimulation. For V2R stimulations, 100 nM AVP was used at the indicated time points. Cells were lysed in radioimmunoprecipitation assay buffer (Sigma) containing a mixture of protease and phosphatase inhibitors (Thermo Fisher Scientific) and clarified by centrifugation. Lysates were resolved on SDS–polyacrylamide gel electrophoresis gels, transferred onto PVDF membranes (Millipore), and probed with appropriate antibodies. Westerns to detect active RAS-GTP were performed using glutathione-Sepharose beads (GE Healthcare) immobilized with the RAS-interactive binding domain of c-Raf-1 fused to glutathione S-transferase as previously described (44). For pERK1/2 ELISA (Sandwich ELISA kit #7177, Cell Signaling Technology), cells were cultured in a 12-well plate, stimulated with indicated concentrations of ligands, and lysed in 150 μl of provided lysis buffer supplemented with protease and phosphatase inhibitors (Thermo Fisher Scientific). ELISA was performed according to the manufacturer's instructions, and absorbance readings were measured on a BioTek Synergy Neo plate reader.

In-Cell Western blot and siRNA RAS-GEF library screen

Cells for In-Cell Western blot were cultured to near confluence in a 96-well plate and stimulated for indicated periods of time with 10 μM isoproterenol, then the medium was discarded, and cells were fixed with 4% formaldehyde in PBS for 20 min at room temperature. Cells were then permeabilized with 0.5% Triton X-100 with 200 mM glycine in PBS for 10 min at room temperature. After washing with PBS, cells were blocked with 3% BSA-PBS for 1 hour at room temperature. The wells were then incubated in primary antibodies diluted in 3% BSA-PBS (rabbit phospho-ERK1/2 at 1:100 and mouse total ERK1/2 at 1:200) overnight at 4°C with gentle rocking. The wells were washed three times with 0.1% Tween 20 in PBS for 10 min at room temperature with gentle shaking. They were then incubated with secondary antibodies diluted in 3% BSA-PBS (LI-COR anti-mouse 680 at 1:1000 and anti-rabbit 800 at 1:1000) for 1 hour at room temperature with gentle rocking and covered with foil to protect from light. The wells were again washed three times with 0.1% Tween 20 in PBS for 10 min at room temperature with gentle shaking and then imaged on the Odyssey imager. The siRNA Ras-GEF library screen was performed using an In-Cell Western screen with knockdown of a library of Ras-GEFs [Life Technologies, D1337830 (custom gene group)] in HEK293 cells expressing FLAG-β$_2$AR in the presence and absence of isoproterenol stimulation (10 μM).

cAMP assays

cAMP accumulation from endogenous β$_2$ARs after isoproterenol stimulation (10 μM) was measured using plasmid pGLO-20F (Promega), which encodes a circularly permuted luciferase cAMP reporter. HEK293 cells were transfected with appropriate siRNAs for 24 hours, followed by a medium change before transfection with pGLO-20F plasmid DNA using Lipofectamine 3000 (Invitrogen) transfection reagent for 24 hours. Cells were then assayed as previously

described (37). For each siRNA treatment, reference wells were treated with 5 μM forskolin, and all experimental cAMP measurements were normalized to the maximum luminescence value measured in the presence of forskolin to control for cell number and DNA transfection efficiencies after siRNA treatment. Another cAMP assay was performed using the HTRF cAMP assay kit from CisBio (cAMP dynamic 2 kit #62AM4PEB) to monitor cAMP levels stimulated by isoproterenol (10 μM) in HEK293 control cells, $G\alpha_s$ KO cells, and $G\alpha_s$ KO cells reconstituted by $G\alpha_s$ transfection. Fluorescence measurements were made using a Victor2 plate reader.

Membrane preparation

HEK293 parental and β-arr1/2 KO cell lines were transfected with FLAG-β2AR DNA, and membranes were harvested 48 hours later at confluence. Membranes were harvested in warm harvesting buffer [0.68 mM EDTA, 150 mM NaCl, and 20 mM Hepes (pH 7.4)] and washed with PBS. Cell suspension was centrifuged for 3 min at 2000 rpm, and the supernatant was removed. Cells were homogenized in cold membrane preparation buffer [10 mM Hepes, 10 mM NaCl, 0.5 mM $MgCl_2$, and 0.5 mM EGTA (pH 7.4)] and centrifuged at 15,000 rpm for 20 min at 4°C. The process was repeated twice, and the supernatant was removed. Cells were resuspended in cold binding assay buffer [10 mM Hepes, 10 mM NaCl, 0.5 mM $MgCl_2$, and 1 mM ascorbic acid (pH 7.4)] and sonicated. Protein concentrations were measured by DC protein assay (Bio-Rad).

Radioligand binding assay

In a polypropylene 96-well plate, binding assay buffer or propranolol (50 μM final for nonspecific binding), [³H]DHAP (2 nM final), and membranes (5 μg per well) were plated in order and incubated for 2 hours at room temperature to reach equilibrium. GF/C filterplates were prepared with 0.3% polyethylenimine to minimize nonspecific binding. Samples were transferred to the filterplates, washed with cold assay buffer, and dried overnight. Each well was counted in MicroScint-0 (PerkinElmer) for 1 min in triplicate.

Statistical analyses

Statistical analyses of data were performed using GraphPad Prism 7 software (GraphPad Software). The data were analyzed by analysis of variance (ANOVA) test or t test. The mean differences of three independent experiments were considered significant when P values were <0.05. Nonlinear regression (least squares fit) analysis was used to fit curves and determine the EC_{50} and E_{max} values.

SUPPLEMENTARY MATERIALS

www.sciencesignaling.org/cgi/content/full/10/484/eaal3395/DC1

Fig. S1. Transferrin uptake experiments and genomic DNA sequencing of the β-arr1 KO cell line.
Fig. S2. Clathrin is important for isoproterenol-mediated β2AR internalization.
Fig. S3. Depletion of both β-arr1 and β-arr2 increases β2AR-mediated cAMP production.
Fig. S4. Sequence of β-arr1/2 double-mutant cells.
Fig. S5. Endogenous β2AR in parental HEK293 and β-arr1/2 KO and β2AR and V2R internalization in these cells.
Fig. S6. β-Arrestin is not required for ERK phosphorylation in arginine vasopressin receptor 2 (V2R)–expressing cells.
Fig. S7. Stable expression of FLAG-β2AR on Gnas f/f MEFs and Gα_s KO cells and effect of EPAC inhibition on isoproterenol-mediated ERK phosphorylation and RAP1A activation.
Fig. S8. EGFR, PI3K, and Gα_i signaling are dispensable for activation of ERK by β2AR, but Gβγ signaling is important.
Movie S1. Live-cell confocal imaging of β2AR internalization in HEK293 cells.
Movie S2. Live-cell confocal imaging of β2AR internalization in β-arr1 KO cells.
Movie S3. Live-cell confocal imaging of β2AR internalization in β-arr–less cells.
Movie S4. Live-cell TIRF imaging of β2AR internalization into clathrin-coated pits in HEK293 cells.

Movie S5. Live-cell TIRF imaging of β2AR internalization into clathrin-coated pits in β-arr1 KO cells.
Movie S6. Live-cell TIRF imaging of β2AR internalization into clathrin-coated pits in β-arr–less cells.

REFERENCES AND NOTES

1. K. L. Pierce, R. T. Premont, R. J. Lefkowitz, Seven-transmembrane receptors. Nat. Rev. Mol. Cell Biol. 3, 639–650 (2002).
2. M. Rask-Andersen, M. S. Almén, H. B. Schiöth, Trends in the exploitation of novel drug targets. Nat. Rev. Drug Discov. 10, 579–590 (2011).
3. S. G. F. Rasmussen, H.-J. Choi, J. J. Fung, E. Pardon, P. Casarosa, P. S. Chae, B. T. DeVree, D. M. Rosenbaum, F. S. Thian, T. S. Kobilka, A. Schnapp, I. Konetzki, R. K. Sunahara, S. H. Gellman, A. Pautsch, J. Steyaert, W. I. Weis, B. K. Kobilka, Structure of a nanobody-stabilized active state of the β2 adrenoceptor. Nature 469, 175–180 (2011).
4. V. V. Gurevich, E. V. Gurevich, The structural basis of arrestin-mediated regulation of G-protein-coupled receptors. Pharmacol. Ther. 110, 465–502 (2006).
5. C. V. Carman, J. L. Benovic, G-protein-coupled receptors: Turn-ons and turn-offs. Curr. Opin. Neurobiol. 8, 335–344 (1998).
6. A. Manglik, T. H. Kim, M. Masureel, C. Altenbach, Z. Yang, D. Hilger, M. T. Lerch, T. S. Kobilka, F. S. Thian, W. L. Hubbell, R. S. Prosser, B. K. Kobilka, Structural insights into the dynamic process of β2-adrenergic receptor signaling. Cell 161, 1101–1111 (2015).
7. R. Nygaard, Y. Zou, R. O. Dror, T. J. Mildorf, D. H. Arlow, A. Manglik, A. C. Pan, C. W. Liu, J. J. Fung, M. P. Bokoch, F. S. Thian, T. S. Kobilka, D. E. Shaw, L. Mueller, R. S. Prosser, B. K. Kobilka, The dynamic process of β2-adrenergic receptor activation. Cell 152, 532–542 (2013).
8. S. K. Shenoy, R. J. Lefkowitz, Seven-transmembrane receptor signaling through β-arrestin. Sci. STKE 2005, cm10 (2005).
9. S. K. Shenoy, R. J. Lefkowitz, β-Arrestin-mediated receptor trafficking and signal transduction. Trends Pharmacol. Sci. 32, 521–533 (2011).
10. S. Ahn, C. D. Nelson, T. R. Garrison, W. E. Miller, R. J. Lefkowitz, Desensitization, internalization, and signaling functions of β-arrestins demonstrated by RNA interference. Proc. Natl. Acad. Sci. U.S.A. 100, 1740–1744 (2003).
11. S. K. Shenoy, M. T. Drake, C. D. Nelson, D. A. Houtz, K. Xiao, S. Madabushi, E. Reiter, R. T. Premont, O. Lichtarge, R. J. Lefkowitz, β-arrestin-dependent, G protein-independent ERK1/2 activation by the β2 adrenergic receptor. J. Biol. Chem. 281, 1261–1273 (2006).
12. J. W. Wisler, S. M. DeWire, E. J. Whalen, J. D. Violin, M. T. Drake, S. Ahn, S. K. Shenoy, R. J. Lefkowitz, A unique mechanism of β-blocker action: Carvedilol stimulates β-arrestin signaling. Proc. Natl. Acad. Sci. U.S.A. 104, 16657–16662 (2007).
13. W. P. Hausdorff, P. T. Campbell, J. Ostrowski, S. S. Yu, M. G. Caron, R. J. Lefkowitz, A small region of the β-adrenergic receptor is selectively involved in its rapid regulation. Proc. Natl. Acad. Sci. U.S.A. 88, 2979–2983 (1991).
14. F. A. Ran, P. D. Hsu, J. Wright, V. Agarwala, D. A. Scott, F. Zhang, Genome engineering using the CRISPR-Cas9 system. Nat. Protoc. 8, 2281–2308 (2013).
15. T. Cermak, E. L. Doyle, M. Christian, L. Wang, Y. Zhang, C. Schmidt, J. A. Baller, N. V. Somia, A. J. Bogdanove, D. F. Voytas, Efficient design and assembly of custom TALEN and other TAL effector-based constructs for DNA targeting. Nucleic Acids Res. 39, e82 (2011).
16. D. A. Conner, M. A. Mathier, R. M. Mortensen, M. Christe, S. F. Vatner, C. E. Seidman, J. G. Seidman, β-Arrestin1 knockout mice appear normal but demonstrate altered cardiac responses to β-adrenergic stimulation. Circ. Res. 81, 1021–1026 (1997).
17. E. V. Gurevich, J. L. Benovic, V. V. Gurevich, Arrestin2 expression selectively increases during neural differentiation. J. Neurochem. 91, 1404–1416 (2004).
18. M. J. Lohse, J. L. Benovic, J. Codina, M. G. Caron, R. J. Lefkowitz, β-Arrestin: A protein that regulates β-adrenergic receptor function. Science 248, 1547–1550 (1990).
19. A. Lochner, J. A. Moolman, The many faces of H89: A review. Cardiovasc. Drug Rev. 24, 261–274 (2006).
20. J. Bain, L. Plater, M. Elliott, N. Shpiro, C. J. Hastie, H. Mclauchlan, I. Klevernic, J. S. C. Arthur, D. R. Alessi, P. Cohen, The selectivity of protein kinase inhibitors: A further update. Biochem. J. 408, 297–315 (2007).
21. R. Iglesias-Bartolome, D. Torres, R. Marone, X. Feng, D. Martin, M. Simaan, M. Chen, L. S. Weinstein, S. S. Taylor, A. A. Molinolo, J. S. Gutkind, Inactivation of a Gα_s-PKA tumour suppressor pathway in skin stem cells initiates basal-cell carcinogenesis. Nat. Cell Biol. 17, 793–803 (2015).
22. K. A. DeFea, J. Zalevsky, M. S. Thoma, O. Déry, R. D. Mullins, N. W. Bunnett, β-Arrestin-dependent endocytosis of proteinase-activated receptor 2 is required for intracellular targeting of activated ERK1/2. J. Cell Biol. 148, 1267–1281 (2000).
23. L. M. Luttrell, F. L. Roudabush, E. W. Choy, W. E. Miller, M. E. Field, K. L. Pierce, R. J. Lefkowitz, Activation and targeting of extracellular signal-regulated kinases by β-arrestin scaffolds. Proc. Natl. Acad. Sci. U.S.A. 98, 2449–2454 (2001).
24. M. Drosten, A. Dhawahir, E. Y. M. Sum, J. Urosevic, C. G. Lechuga, L. M. Esteban, E. Castellano, C. Guerra, E. Santos, M. Barbacid, Genetic analysis of Ras signalling pathways in cell proliferation, migration and survival. EMBO J. 29, 1091–1104 (2010).

25. A. Fernández-Medarde, E. Santos, The RasGrf family of mammalian guanine nucleotide exchange factors. *Biochim. Biophys. Acta* **1815**, 170–188 (2011).

26. W. J. Koch, J. Inglese, W. C. Stone, R. J. Lefkowitz, The binding site for the βγ subunits of heterotrimeric G proteins on the β-adrenergic receptor kinase. *J. Biol. Chem.* **268**, 8256–8260 (1993).

27. L. M. Luttrell, R. J. Lefkowitz, The role of β-arrestins in the termination and transduction of G-protein-coupled receptor signals. *J. Cell Sci.* **115**, 455–465 (2002).

28. T. A. Kohout, F. S. Lin, S. J. Perry, D. A. Conner, R. J. Lefkowitz, β-Arrestin 1 and 2 differentially regulate heptahelical receptor signaling and trafficking. *Proc. Natl. Acad. Sci. U.S.A.* **98**, 1601–1606 (2001).

29. Y.-C. Ma, J. Huang, S. Ali, W. Lowry, X.-Y. Huang, Src tyrosine kinase is a novel direct effector of G proteins. *Cell* **102**, 635–646 (2000).

30. J. M. Schmitt, P. J. Stork, Gα and Gβγ require distinct Src-dependent pathways to activate Rap1 and Ras. *J. Biol. Chem.* **277**, 43024–43032 (2002).

31. K. L. Pierce, R. J. Lefkowitz, Classical and new roles of β-arrestins in the regulation of G-PROTEIN-COUPLED receptors. *Nat. Rev. Neurosci.* **2**, 727–733 (2001).

32. E. Alvarez-Curto, A. Inoue, L. Jenkins, S. Zahir Raihan, R. Prihandoko, A. B. Tobin, G. Milligan, Targeted elimination of G proteins and arrestins defines their specific contributions to both intensity and duration of G protein-coupled receptor signaling. *J. Biol. Chem.* **291**, 27147–27159 (2016).

33. Q. Wang, J. Zhao, A. E. Brady, J. Feng, P. B. Allen, R. J. Lefkowitz, P. Greengard, L. E. Limbird, Spinophilin blocks arrestin actions in vitro and in vivo at G protein-coupled receptors. *Science* **304**, 1940–1944 (2004).

34. J. Luo, J. M. Busillo, J. L. Benovic, M₃ muscarinic acetylcholine receptor-mediated signaling is regulated by distinct mechanisms. *Mol. Pharmacol.* **74**, 338–347 (2008).

35. A. R. B. Thomsen, B. Plouffe, T. J. Cahill III, A. K. Shukla, J. T. Tarrasch, A. M. Dosey, A. W. Kahsai, R. T. Strachan, B. Pani, J. P. Mahoney, L. Huang, B. Breton, F. M. Heydenreich, R. K. Sunahara, G. Skiniotis, M. Bouvier, R. J. Lefkowitz, GPCR-G protein-β-arrestin super-complex mediates sustained G protein signaling. *Cell* **166**, 907–919 (2016).

36. J. P. Vilardaga, F. G. Jean-Alphonse, T. J. Gardella, Endosomal generation of cAMP in GPCR signaling. *Nat. Chem. Biol.* **10**, 700–706 (2014).

37. R. Irannejad, J. C. Tomshine, J. R. Tomshine, M. Chevalier, J. P. Mahoney, J. Steyaert, S. G. F. Rasmussen, R. K. Sunahara, H. El-Samad, B. Huang, M. von Zastrow, Conformational biosensors reveal GPCR signalling from endosomes. *Nature* **495**, 534–538 (2013).

38. J. F. Hancock, Ras proteins: Different signals from different locations. *Nat. Rev. Mol. Cell Biol.* **4**, 373–384 (2003).

39. K. Eichel, D. Jullie, M. von Zastrow, β-Arrestin drives MAP kinase signalling from clathrin-coated structures after GPCR dissociation. *Nat. Cell Biol.* **18**, 303–310 (2016).

40. C. J. Merrifield, M. E. Feldman, L. Wan, W. Almers, Imaging actin and dynamin recruitment during invagination of single clathrin-coated pits. *Nat. Cell Biol.* **4**, 691–698 (2002).

41. J. B. Regard, N. Cherman, D. Palmer, S. A. Kuznetsov, F. S. Celi, J.-M. Guettier, M. Chen, N. Bhattacharyya, J. Wess, S. R. Coughlin, L. S. Weinstein, M. T. Collins, P. G. Robey, Y. Yang, Wnt/β-catenin signaling is differentially regulated by Gα proteins and contributes to fibrous dysplasia. *Proc. Natl. Acad. Sci. U.S.A.* **108**, 20101–20106 (2011).

42. W. Stallaert, E. T. van der Westhuizen, A.-M. Schönegge, B. Plouffe, M. Hogue, V. Lukashova, A. Inoue, S. Ishida, J. Aoki, C. Le Gouill, M. Bouvier, Purinergic receptor transactivation by the β₂-adrenergic receptor increases intracellular Ca²⁺ in non-excitable cells. *Mol. Pharmacol.* **91**, 533–544 (2017).

43. R. Schrage, A.-L. Schmitz, E. Gaffal, S. Annala, S. Kehraus, D. Wenzel, K. M. Büllesbach, T. Bald, A. Inoue, Y. Shinjo, S. Galandrin, N. Shridhar, M. Hesse, M. Grundmann, N. Merten, T. H. Charpentier, M. Martz, A. J. Butcher, T. Slodczyk, S. Armando, M. Effern, Y. Namkung, L. Jenkins, V. Horn, A. Stößel, H. Dargatz, D. Tietze, D. Imhof, C. Galés, C. Drewke, C. E. Müller, M. Hölzel, G. Milligan, A. B. Tobin, J. Gomeza, H. G. Dohlman, T. K. Harden, M. Bouvier, S. A. Laporte, J. Aoki, B. K. Fleischmann, K. Mohr, G. M. König, T. Tüting, E. Kostenis, The experimental power of FR900359 to study Gq-regulated biological processes. *Nat. Commun.* **6**, 10156 (2015).

44. J.-J. Chen, C. M. Mikelis, Y. Zhang, J. S. Gutkind, B. Zhang, TRAIL induces apoptosis in oral squamous carcinoma cells: A crosstalk with oncogenic Ras regulated cell surface expression of death receptor 5. *Oncotarget* **4**, 206–217 (2013).

Citation: M. O'Hayre, K. Eichel, S. Avino, X. Zhao, D. J. Steffen, X. Feng, K. Kawakami, J. Aoki, K. Messer, R. Sunahara, A. Inoue, M. von Zastrow, J. S. Gutkind, Genetic evidence that β-arrestins are dispensable for the initiation of β₂-adrenergic receptor signaling to ERK. *Sci. Signal.* **10**, eaal3395 (2017).

Science Signaling

Genetic evidence that β-arrestins are dispensable for the initiation of β$_2$-adrenergic receptor signaling to ERK

Morgan O'Hayre, Kelsie Eichel, Silvia Avino, Xuefeng Zhao, Dana J. Steffen, Xiaodong Feng, Kouki Kawakami, Junken Aoki, Karen Messer, Roger Sunahara, Asuka Inoue, Mark von Zastrow and J. Silvio Gutkind

β-Arrestins not necessary

The β$_2$-adrenergic receptor is thought to activate signaling mediated by the kinase ERK through a pathway that does not require G proteins but rather the β-arrestin family of scaffolding proteins. Biased agonists for the β$_2$-adrenergic receptor are being developed to selectively activate this pathway. O'Hayre *et al.* took advantage of improved technologies for knocking out proteins in cells and unexpectedly found that β-arrestins were not required for ERK activation downstream of the β$_2$-adrenergic receptor, although β-arrestin 2 was required for receptor internalization. Instead, the pathway depended on G α$_s$, Gβγ, and various other signaling molecules. These results suggest that biased agonists for the β$_2$-adrenergic receptor may exert their effects in a β-arrestin–independent manner.

ARTICLE TOOLS	http://stke.sciencemag.org/content/10/484/eaal3395
SUPPLEMENTARY MATERIALS	http://stke.sciencemag.org/content/suppl/2017/06/16/10.484.eaal3395.DC1
RELATED CONTENT	http://stke.sciencemag.org/content/sigtrans/9/456/ra117.full http://stke.sciencemag.org/content/sigtrans/10/471/eaah5756.full http://stke.sciencemag.org/content/sigtrans/7/310/pe3.full http://stke.sciencemag.org/content/sigtrans/8/405/ra123.full http://stke.sciencemag.org/content/sigtrans/4/185/ra51.full http://stke.sciencemag.org/content/sigtrans/3/125/ra46.full http://stke.sciencemag.org/content/sigtrans/5/221/ra33.full http://stke.sciencemag.org/content/sigtrans/9/424/ra39.full http://stke.sciencemag.org/content/sigtrans/8/389/ra79.full http://science.sciencemag.org/content/sci/340/6132/615.full http://science.sciencemag.org/content/sci/335/6072/1055.full http://science.sciencemag.org/content/sci/259/5096/825.full.pdf http://science.sciencemag.org/content/sci/335/6072/1106.full http://science.sciencemag.org/content/sci/260/5116/1910.full.pdf http://science.sciencemag.org/content/sci/248/4962/1547.full.pdf http://science.sciencemag.org/content/sci/283/5402/655.full http://science.sciencemag.org/content/sci/271/5247/363.full.pdf http://stm.sciencemag.org/content/scitransmed/1/1/1ra1.full file:/content http://stke.sciencemag.org/content/sigtrans/10/487/eaao3019.full http://stke.sciencemag.org/content/sigtrans/10/494/eaap7677.full http://stke.sciencemag.org/content/sigtrans/10/498/eaao3332.full http://stke.sciencemag.org/content/sigtrans/11/518/eaan3714.full http://stke.sciencemag.org/content/sigtrans/11/519/eaat0494.full

Use of this article is subject to the Terms of Service